Hindawi
Geofluids
Volume 2020, Article ID 9426586, 14 pages
https://doi.org/10.1155/2020/9426586

Research Article

Relationship between Tectonism and Composition and Pore Characteristics of Shale Reservoirs

Fuhua Shang[1,2,3] **Yanming Zhu**[1,2] **Haitao Gao**[1,2] **Yang Wang**[1,2] **and Ruiyin Liu**[4]

[1]*Key Laboratory of Coalbed Methane Resource & Reservoir Formation Process, Ministry of Education, China University of Mining and Technology, Xuzhou 221008, China*
[2]*School of Resources and Earth Science, China University of Mining and Technology, Xuzhou 221116, China*
[3]*Department of Earth and Environmental Sciences, The University of Texas at Arlington, Arlington, TX 76019, USA*
[4]*State Key Laboratory of Oil and Gas Reservoir Geology and Exploitation, Chengdu University of Technology, Chengdu 610059, China*

Correspondence should be addressed to Yanming Zhu; ts14010087@cumt.edu.cn

Received 21 October 2019; Revised 20 December 2019; Accepted 30 January 2020; Published 20 February 2020

Academic Editor: Fausto Grassa

Tectonism is one of the major controlling factors of shale gas accumulation and enrichment in China. To explore the relationship between tectonism and composition and pore characteristics of shale reservoirs, this research carried out mineralogy tests, organic geochemistry tests, field emission scanning electron microscopy (FE-SEM) experiments, and low-pressure gas adsorption (LPGA, N_2 and CO_2) experiments on the shale samples of various deformation intensities from Southwestern China. Based on the FE-SEM image analyses, it can be found that there are large differences in pore characteristics in shale samples with different deformation intensities. The samples with strong deformation have more organic pores, mainly related to the clay-organic aggregates and rigid grains. Tectonism can cause organic matter (OM) and clay minerals to be mixed or OM to fill in the clay layers, resulting in the retention of some organic pores. It is the presence of pressure shadows around the rigid grains that can resist tectonic extrusion and protect some organic pores. LPGA experiment results also show that micropore-specific surface areas and pore volumes of the samples with strong deformation are larger than those with weak deformation. The shale samples with strong deformation also have more microchannels and microfractures. Tectonism can also cause some micropores to become macropores; for example, tectonism can cause the rigid grains to slide and rotate, enlarging the dissolution pores at the edges of rigid grains. Shale samples with strong deformation have a smaller mesopore volume; but due to the presence of organic-clay aggregates, a larger mesopore-specific surface area embarks on these samples. According to fractal dimension calculations, it is found that in strong deformed shale, more multiple dimensions of the pore system tend to represent rougher pore surfaces and more irregular shapes. Besides, rougher pore surfaces are eager to provide more adsorption sites and enhance the adsorption capacity of the deformed shale. This study investigates the relationship between tectonism and composition and pore characteristics of shale reservoirs and may promote understanding of the accumulation of shale gas in highly deformed areas.

1. Introduction

Shale gas, taken as a very important unconventional natural gas, is essential to oil and gas production. Shale gas is mainly stored in pores and fractures in the state of free gas or as gas adsorbed onto kerogen and clay particle surface [1–4]. The pore structure strikes a remarkable impact on the gas storage and flow capacity of shale [5–13]. Unlike the gas shale field in the United States, the marine shale in Southern China has experienced multiple tectonism, as tectonism has been

regarded as one of the most important factors affecting the shale pore structure and gas occurrence state [4, 14–17]. Nowadays, more and more Chinese researchers have approved such viewpoints that tectonics is the key factor for shale gas accumulation in shale, and they set about conducting extensive research on tectonics in gas shale area [18–31]. However, the relationship between tectonism and composition and pore characteristics of shale reservoirs is still unclear.

Two main ways can be observed concerning the influence of tectonism on the reservoir, namely, the vertical burial and uplift of the stratum and the extrusion and tension on the plane [4, 18, 23, 26]. And tectonism can also cause changes in minerals, especially clay minerals and OM [32–34]. Therefore, tectonism can change the pores and fractures of shale reservoirs by stress and heat stress, which then further alters the occurrence of shale gas [18, 23, 34, 35]. Multistage tectonism together with dramatic changes in the pore structure took place in some shale-deposited zones in Sichuan Basin, Southwestern China [21, 23–27]. Therefore, it is important to figure out the relationship between tectonism and pore structure. It is worth noting that there are still many controversies about the relationship between tectonic stress and the pore volume and specific surface area of shale. Some scholars believe that tectonic stress will cause the reduction of pores; that is, as the tectonism increases, the degree of pore reduction will increase, especially for mesopores and macropores [4, 23]. However, it is argued among experts that the tectonism can also produce the cleavage domains and increase the pore volume and specific surface area [32, 36]. Ma et al. found that the Lujiaping shale developed three-dimensional connected pore systems composed of nanometer-sized intergranular pore spaces, aggregate pore spaces in clay flakes, and a pore network in the cleavage domains, which provides the main specific surface area and adsorption point [32]. Although researchers pay more and more attention to the role of tectonism in shale gas accumulation, there exist many blurry doubts and unsolved issues such as the mechanism of the influence of tectonism on reservoir pore structure, which needs further research.

Recently, some researchers have got down to notice natural tectonic deformed samples and conducted experiments to study the relationship between tectonism and shale composition and pore structure features through experiments [32, 36–40]. Ju et al. made inner comparison among the material composition and pore characteristics of brittle deformation, ductile deformation, and brittle-ductile shale samples from various areas and found that brittle shear results in microfractures and large pores and thus has an impact on the desorption and percolation capability of shale gas; the ductile deformation increased the specific surface area and enhanced the adsorption capacity of deformed shale [36]. Liang et al. found that the tectonism has little effect on shale mineral composition, maturity, porosity, and total pore volume by comparing the deformed sample with the undeformed sample but has a great influence on specific surface area, adsorption capacity, and pore size distribution [38]. Zhu et al. pointed out that the pores and microfracture systems will be combined during the deformation process so that these open pores become good reservoir space and migration channel [37, 39]. This study is of far-reaching importance of guiding the future exploration and development of structural regions, especially the weaker one.

2. Materials and Methods

2.1. Sample Selection. All samples were collected from the Lower Cambrian Lujiaping Formation in the Changzhang region. Located in the Dabashan thrust belt and undergone multistage tectonic movements, the Changzhang region is the cradle of anticline structures [41, 42]. The samples were all taken from a symmetrical anticline, and the deformation intensity is weakened from the core to the two wings (Figure 1). Based on the macroscopic characteristics, including hardness, scratch, rubbing mirrors, and deformation intensity, the samples were divided into strong deformed shale and weak deformed shale. Strong deformed samples include CZ-4, CZ-5, and CZ6, and weak deformed samples include CZ-1 to CZ-3 and CZ-7 to CZ-8.

2.2. Petrophysical Test. The samples were crushed to below 60 mesh. TOC content test and mineral composition test were measured by a LECO CS230 carbon and sulfur analyzer and Rigaku D/Max-3B diffractometer, respectively. The experiments were conducted in accordance with Chinese national standards GB/T19145-2003 and SY/T5163-2010. The whole rock analysis and clay minerals were estimated by semiquantitative mineral spectrum. Both experiments were carried out at Experimental Research Center of East China Branch, Sinopec.

The equivalent vitrinite reflectance test (*Ro*) was measured by 3Y-Leica DMR XP microscopy equipped with a microphotometer, and the results were analyzed in the Key Laboratory of Coalbed Methane Resources and Reservoir Formation Process of the Ministry of Education (CUMT). Owing to the deficiency in vitrinite in the Lower Cambrian Lujiaping Formation shale, the *Ro* is converted into vitrinite-like material reflectance (*Rom*) by calculation [43].

2.3. FE-SEM Experiment. The samples were processed by argon ion beam and then sprayed with 1 mm thick gold. The FE-SEM experiment was performed at the Jiangsu Design Institute of Geology for Minerals Resources, taking use of FE-SEM (Quanta 200F) equipped with an energy-dispersive spectrometer (EDS) to identify the mineral types and help identify pore types. These analyses were presented at the temperature of 24°C with the humidity level of 35%.

2.4. Low-Pressure Gas Adsorption (LPGA). LPGA experiments were strictly performed at the Physical and Chemical Center of Beijing, according to the Chinese National Standard GB/T 19587-2004. All experimental samples were smashed to 40-60 mesh, and then, were automatically degassed under a vacuum of ~110° for more than 16 h. The instrument used was called the Micromeritics ASAP

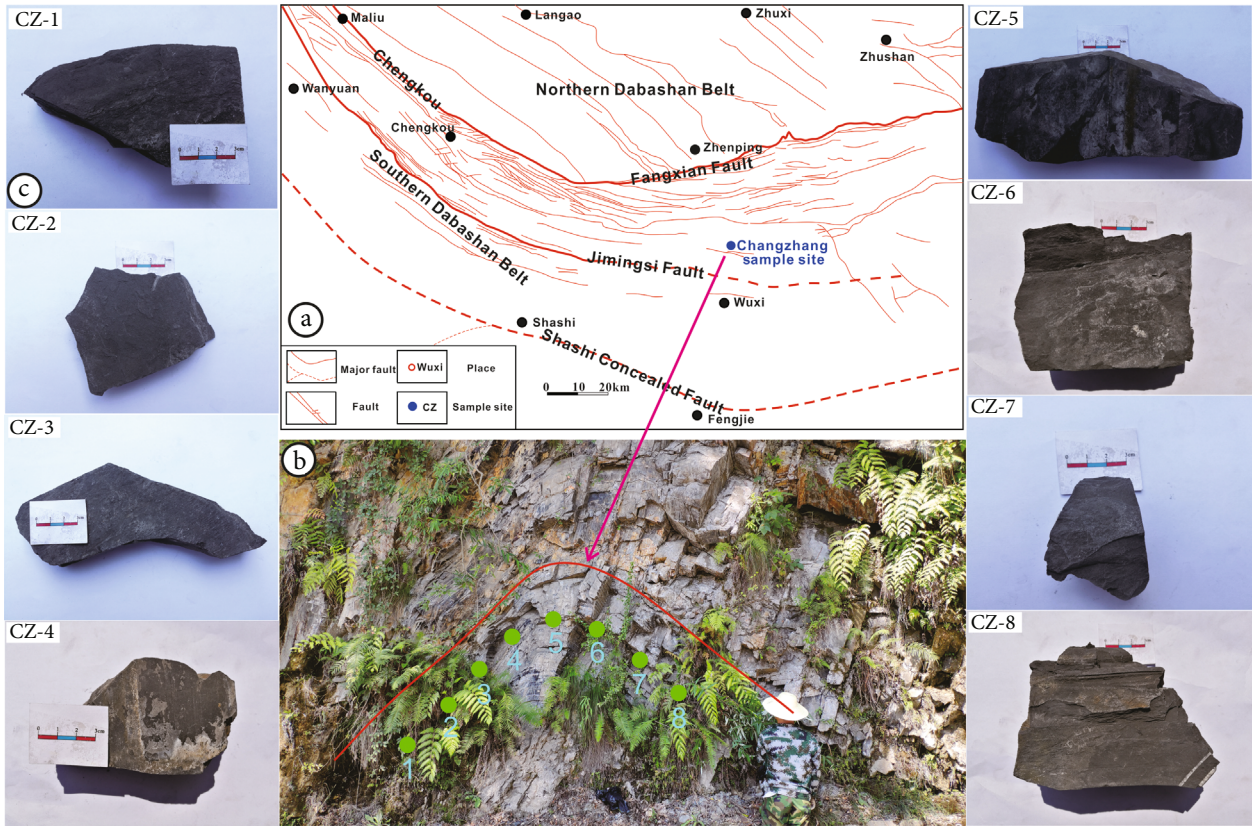

Figure 1: (a) Geographic location and structure of the study region in the northeast Chongqing. (b) Outcrops and the structural deformation characteristics of samples in the Changzhang region. The anticline is well exposed, and the two wings are basically symmetrical, showing good deformation characteristics. (c) Sample information, the samples in anticline core have the strongest deformation. Modified from Hu et al. [41] and Shi et al. [42].

2020 HD88 analyzer. N_2 adsorption experiment was implemented in the bath temperature of -196°C (77 K) under the relative pressure (P/P_0) ranging from 0.009 to 0.995. And the bath temperature in CO_2 adsorption experiment is 0°C (273 K), and the relative pressure (P/P_0) of CO_2 adsorption range is between 0.0001 and 0.032. The experiment data of LPGA experiment were interpreted by the field density functional theory (DFT) model for pore size distribution of the shale.

2.5. Method of Fractal Calculation. The fractal dimensions were calculated based on the data obtained from LP-N_2-GA experiment. The equation is as follows:

$$\frac{V}{V_m} = c \times \left[RT \times \ln\left(\frac{P_0}{P}\right)\right]^{-1/s}, \quad (1)$$

where V is the adsorbed gas volume at the equilibrium pressure (P), V_m is the monolayer coverage volume, c is a characteristic constant, R is the universal gas constant, T is the absolute temperature, P_0 is the saturated vapor pressure, and the parameter of s depends on fractal dimensions and the specific mechanism of gas adsorption.

Equation (1) can be written in log-log terms:

$$\ln V = \text{const} + s \times \ln\left[\ln\left(\frac{P_0}{P}\right)\right]. \quad (2)$$

According to the fractal FHH theory, the regression straight slope (s) of $\ln V$ can be used to calculate fractal dimensions D:

$$D = s + 3. \quad (3)$$

3. Results

3.1. Geochemical and Mineralogical Characterization of Different Shale Samples. The geochemical and mineralogical data for all samples are shown in Table 1. The TOC contents of the Lujiaping shale scope from 1.01% to 1.79% with average values of 1.35%. The *Ro* values between 3.93% and 4.05% are calculated with the mean of 3.98%, and all the samples are in the overmature stage.

The XRD data have proven that quartz and clay are examined to be the dominant minerals as their overall contents occupy more than 55%. Specifically, the content of quartz is usually relatively high, between 30.1% and 48.8% with average values of 40.1% (Table 1). All the

Table 1: Geochemistry and mineral composition of the Lujiaping shale.

Sample ID	Features of sample	Quartz (%)	Feldspar (%)	Carbonates (%)	Clays (%)	Pyrite (%)	Chlorite (%)	Illite (%)	I/S (%)	TOC (%)	*Ro* (%)
CZ-1	Weak deformed	34.0	13.2	20.3	23.3	1.8	46	50	4	1.0	4.03
CZ-2	Weak deformed	30.1	14.5	25.8	23.2	1.8	38	53	9	1.0	3.95
CZ-3	Weak deformed	31.5	13.2	22.5	27	1.1	34	58	8	1.4	3.97
CZ-4	Strong deformed	48.7	17.1	8.1	19.1	2.6	20	72	8	1.8	3.98
CZ-5	Strong deformed	40.1	16.4	15	22.7	2.3	37	55	8	1.2	3.99
CZ-6	Strong deformed	48.8	14.4	6.4	22.9	4	40	53	7	1.7	3.93
CZ-7	Weak deformed	42.9	15.7	6.1	27.7	3.6	36	56	8	1.5	3.99
CZ-8	Weak deformed	44.7	15	5.3	27.4	4	29	62	9	1.5	4.05

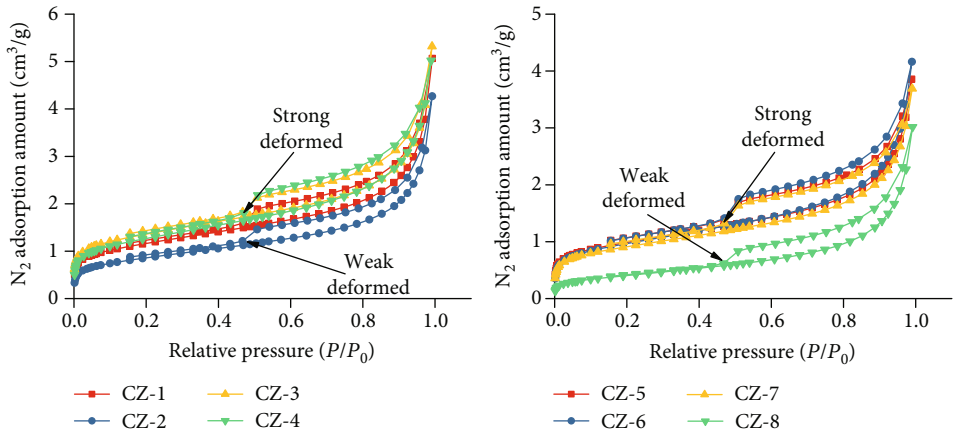

Figure 2: N_2 adsorption-desorption isotherms of the Lujiaping shale.

Lujiaping shales boast a certain amount of carbonate, feldspar, and pyrite with greatly varied contents seen from different samples. It is worth noting that the clay mineral content ranged from 19.1% to 27.7% with a mean value of 24.2%. The illite and chlorite represent the primary clay minerals, and the former contents of which scope from 50% to 72% of total clay content with a mean value of 57.4%. The total amount of quartz and clay of the CZ-4 and CZ-6 with strong deformation can reach about 70%; in particular, the quartz content is much higher than other samples.

3.2. Pore Structure Analyses with the LPGA. Figure 2 shows the N_2 adsorption-desorption isotherm of the selected deformed shale samples. Combining with previous studies, obviously, to summarize the pore morphology characteristics in shale can be inferred based on the type of N_2 adsorption-desorption isotherm and the shape of the hysteresis loop [8, 11, 44]. In accordance with the IUPAC classification of the hysteresis loops, the N_2 adsorption-desorption isotherm of the shale samples belongs to Types H2 and H3 [11, 45–48]. It can be seen that the N_2 adsorption-desorption isotherm of strong deformed samples has large hysteresis loops (Type H2), indicating that these samples contain a large number of ink bottle-shaped pores. The N_2 adsorption-desorption isotherm of the weak deformed samples (CZ-2 and CZ-8) is similar to Type H3, indicating that these samples contain slit-like pores. These pores may be related to the plate structure of clay particles, which are usually flat in the SEM images. What should be paid attention is that the hysteresis loop of N_2 adsorption is a superposition of multiple standard loops and is also a manifestation of the complex pore structure characteristics of the samples.

Figure 3 is the CO_2 adsorption isotherms of all shale samples, typically as the I adsorption isotherms. Shale samples with various deformation intensities have a significant difference in carbon dioxide adsorption capacities. In CZ-6, CO_2 adsorption is seen as the largest amount while the smallest amount in the CZ-1. In general, the shale samples with strong deformation have a larger adsorption

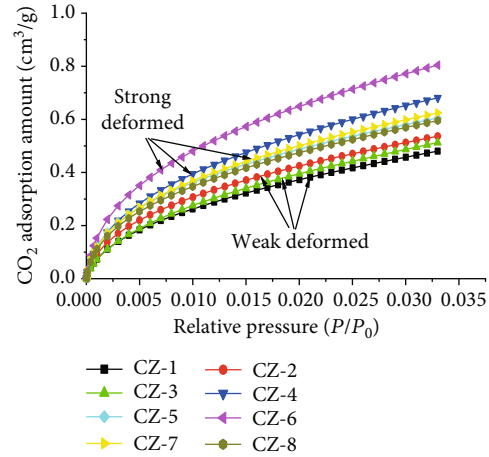

Figure 3: CO_2 adsorption isotherms of the Lujiaping shale.

amount. The relationship between the pressure and the CO_2 adsorption amount of these samples can be converted into the differences in specific surface area and micropore volume.

The pore volume and specific surface area of these samples were calculated by the DFT model using the N_2 and CO_2 adsorption data (Table 2). Figure 4 shows that micropores and mesopores contribute to the major pore volume, which can reach almost 80%. The total pore volume is mainly contributed by pores smaller than 2 nm and 10-50 nm, and pores of other pore sizes also contribute a part of the pore volume. And it can be found that the pore volume contributed by the micropores in CZ-4, CZ-5, and CZ-6 with strong tectonic deformation is larger than that of the mesopores. Conversely, in other samples with weak deformation, the mesopores contribute more to the pore volume. Surprisingly, pores of 2-10 nm are not well developed in these samples and may be related to the tectonism.

Figure 5 shows that in all samples, the specific surface area gradually decreased as the pore size increased. The specific surface area is mainly contributed by the micropores, which provide up to 70% of the total specific surface area.

Table 2: Total PV and SSA of the Lujiaping shale from the data of LPGA experiments.

Sample ID	Total PV of gas absorption (μl/g)			Total SSA of gas absorption (m^2/g)		
	Micropore	Mesopore	Macropore	Micropore	Mesopore	Macropore
CZ-1	1.29	3.91	2.15	3.11	1.06	0.10
CZ-2	1.15	3.39	1.91	3.07	0.90	0.09
CZ-3	1.42	4.08	2.07	3.33	1.12	0.10
CZ-4	1.64	4.25	1.50	4.20	1.18	0.07
CZ-5	1.54	3.32	1.12	4.06	0.93	0.05
CZ-6	1.62	3.68	1.26	4.60	1.03	0.06
CZ-7	1.33	3.20	1.10	3.64	0.91	0.05
CZ-8	1.02	2.84	1.24	3.06	0.70	0.06

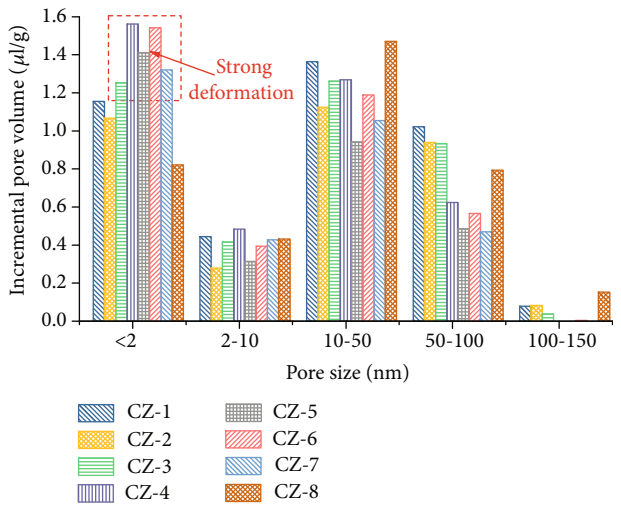

Figure 4: Pore volume distribution of the Lujiaping shale from the data of LPGA experiments.

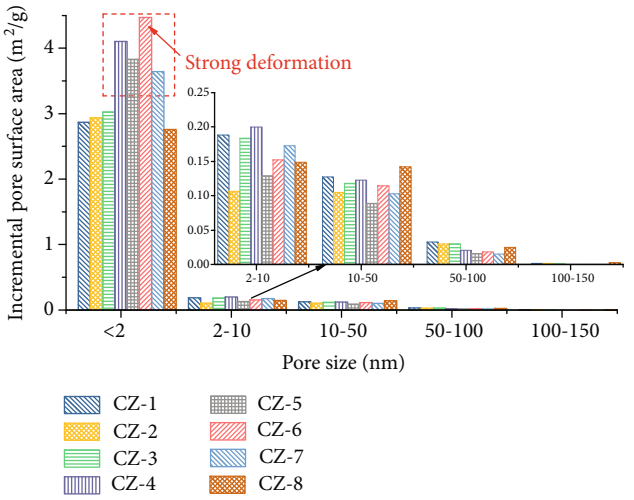

Figure 5: Pore surface distribution of the Lujiaping shale from the data of LPGA experiments.

Although the total specific surface area of all samples is created by micropores, the micropores in the strong deformed shale samples provide more specific surface area.

3.3. Pore Morphology Analyses Based on FE-SEM Images. Shale has a variety of pore types, and each pore type has a complex morphology and origin [4, 8–13, 49–51]. In recent years, some researchers have used FE-SEM experiments to observe the appearance and pore types of shale pores but rarely observed the pore characteristics in the deformed shale samples [9, 11–13]. FE-SEM observation of the pore characteristics of the Lujiaping Formation shale reveals that there are significant variations in the pore characteristics of the samples among various deformation intensities. The tectonism has a significant influence on OM pores, interP pores, and microchannels and microfractures, and the differences among these pores are emphasized.

There are relatively few OM pores in most samples (Figures 6(a)–6(d)), which is consistent with previous research results, probably due to the overmature stage of the Lujiaping Formation and related to strong compaction of tectonic deformation [32, 37, 50]. The weak deformed shale is possessed with some scattered organic pores and microfractures at the edges of OM and clay minerals (Figure 6(a)). However, comparatively more OM pores in the strong deformed shale samples are mainly associated with the OM-clay aggregate and the supporting effect of rigid grains (Figures 6(c) and 6(d)). Multiple types of interP pores can be seen in the SEM images, which have different shapes and sizes and vary greatly (Figures 6(e)–6(h)). It shows that there are usually interP pores between OM and clay minerals (Figure 6(a)). These pores are generally large in length and can effectively improve the pore connectivity. InterP pores are always closely related to rigid grains (quartz, carbonate, feldspar, and mica), especially around rigid grains (Figures 6(e)–6(h)). There are always some triangular regions at the junction of rigid grains and other minerals. These interP pores are either irregular in shape or nearly rectangular outlines due to the structure of the rigid grains (Figures 6(f) and 6(h)).

SEM images also reveal that there are more porous OM pores between the pyrite framboids, although these organic pores are small, but the number is relatively large (Figure 6(c)). For one aspect, it may be due to the tectonic compaction that many pyrite grains are loose from the surrounding clay, resulting in some interP pores

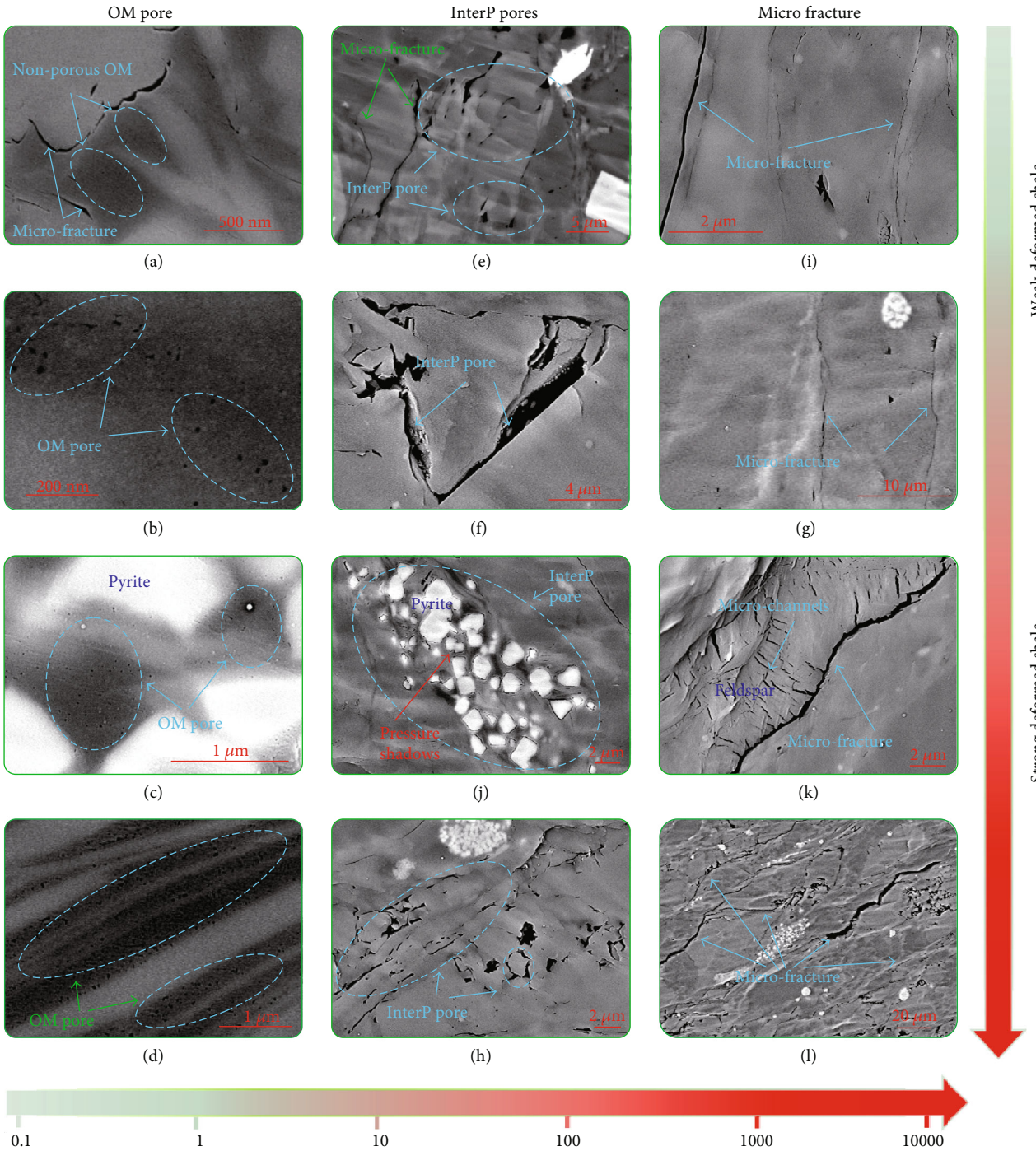

FIGURE 6: Example of pores within the Lujiaping shale. (a, b) SEM images show that most samples contain few OM pores. (c) OM between pyrite grain has more organic pores. (d) The OM-clay aggregate in the strong deformed samples contains some organic pores. (e) Triangular interP pores occur on the edge of rigid grains. (f) InterP pores around the rigid grains. (j) InterP pores between pyrite grain and OM and clay. (h) Long strip-shaped interP pore around the rigid grains. (i, g) Microfractures developed around minerals are generally small. (k) Microchannels occur mostly inside the grain and perpendicular to the edges of the particles, while microfractures are mostly along the edges of the particles. (l) Microchannels and microfractures related to deformation, and the size is relatively large.

(Figure 6(j)). Microfractures and microchannels are typically linear, with lengths between nanometers and micrometers. For another aspect, microfractures are usually cut along the edges of grains, whereas microchannels are usually perpendicular to the plane (Figures 6(i)–6(l)). The microfractures generally feature better connectivity and larger size than those of the microchannels. The multistage tectonic movements developed more microchannels and microfractures. The strong deformed shale samples have more microchannels and microfractures. In the meantime,

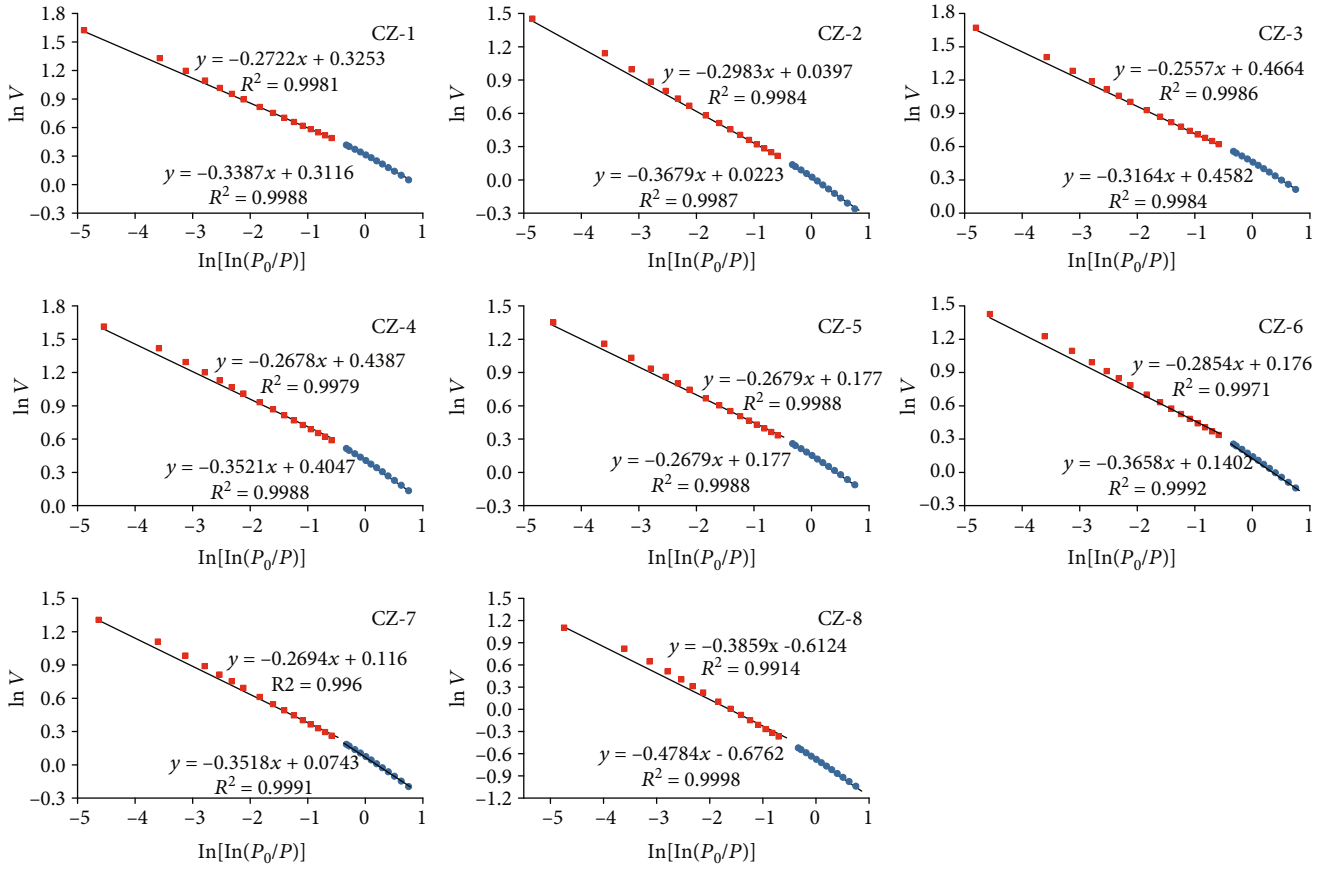

Figure 7: Fractal fitting curves of the Lujiaping shale.

Table 3: Fractal dimensions of the Lujiaping shale.

Sample ID	P/P_0: 0-0.5			P/P_0: 0.5-1		
	K_1	$D_1 = 3 + K_1$	R^2	K_2	$D_2 = 3 + K_2$	R^2
CZ-1	-0.3387	2.6613	0.9988	-0.2722	2.7278	0.9981
CZ-2	-0.3679	2.6321	0.9987	-0.2983	2.7017	0.9984
CZ-3	-0.3164	2.6836	0.9984	-0.2557	2.7443	0.9986
CZ-4	-0.3521	2.6479	0.9988	-0.2678	2.7322	0.9979
CZ-5	-0.3427	2.6573	0.999	-0.2679	2.7321	0.9988
CZ-6	-0.3658	2.6342	0.9992	-0.2854	2.7146	0.9971
CZ-7	-0.3518	2.6482	0.9991	-0.2694	2.7306	0.996
CZ-8	-0.4784	2.5216	0.9998	-0.3859	2.6141	0.9914

these microchannels and microfractures play a key role in shale gas migration and storage. They can increase porosity and permeability and contribute to later fracturing production [1, 51].

3.4. Fractal Characteristics of Pores in Deformed Shale. The fractal curves of the shale samples are similar, but there are some differences in the slopes of the liner fitting lines (Figure 7). The fractal dimension of all samples obtained from the FHH model using nitrogen adsorption is mentioned in Table 2. Each sample has two fractal dimensions, including P/P_0 at 0-0.5 and 0.5-1. The slopes of the correlation curves of the two parts are different, and the correlation coefficient is greater than 0.99. This phenomenon may be caused by different mechanisms of nitrogen adsorption at diverse stages. The linear regression values K_1 and K_2 and the correlation coefficients D_1 and D_2 of the correlation curve are included in Table 3.

D_1 represents the fractal dimension of the relatively small nanopore in the low-pressure stage ($P/P_0 < 0.5$), while D_2 represents the fractal dimension of the relatively large nanopore in the high-pressure stage ($P/P_0 > 0.5$). And D_1 is between 2.5216 and 2.6836, with an average of 2.6357. D_2 is between 2.6141 and 2.7443, and the average is 2.7122. According to Table 2 and Figure 7, it can be found that D_2 is usually larger than D_1. Strong deformed samples generally

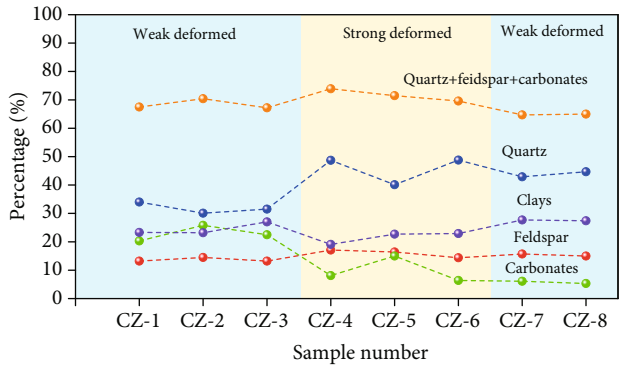

Figure 8: Mineral composition of the Lujiaping shale.

have relatively larger D_1 and D_2, suggesting that tectonism makes the pores in the shale more complex, especially for relatively large nanopores.

4. Discussion

4.1. Effect of Tectonism on Shale Composition. The primary compositions of organic-rich shale embrace OM, clay minerals, and brittle minerals, such as quartz, feldspar, carbonate, and pyrite. There are many factors which can affect the composition of shale, including material sources, sedimentary environment, diagenesis, and tectonism [2, 4, 7, 13, 36]. According to Table 1, all samples collected from the Lujiaping Formation shale in the Changzhang region generally contain relatively high TOC and brittle mineral contents. Previous studies have shown that brittle deformed shale (BDS) samples always contain relatively high TOC and brittle mineral content, while ductile deformed shale (DDS) samples generally have higher clay mineral content [36–39]. However, this conclusion is not very consistent with the XRD results of the deformed samples in the Changzhang region. Shale samples with strong deformation generally have high quartz content and relatively low clay mineral content than samples with weak deformed shale samples (Figure 8).

In fact, tectonism can change the diagenetic stage by stress and heat stress and thus change the composition of shale. On the one hand, as the buried depth increases and the diagenesis strengthens, some unstable minerals will be transformed into other minerals [45]. For example, feldspar will be transformed into quartz and kaolinite under the action of organic acid [52]. On the other hand, extrusion and tension on the plane can change the stress structure of the reservoir by forming different structural styles, and the microstructure and chemical composition of minerals of the shale were changed to a large extent [23, 26, 31, 53]. Ramsay first analyzed the anticline fold and its internal strain characteristics, finding that the stratum above the neutral plane exhibits tensile stress and the stratum below the neutral plane exhibits compressive stress (Figure 9). During the process of stress extrusion to form an anticline, the part above the neutral surface of the Lujiaping shale will be subjected to strong tensile stress, which will change the composition of the shale [33–35, 52–54]. As shown in Figure 6, under tensile stress, more ductile clay and OM

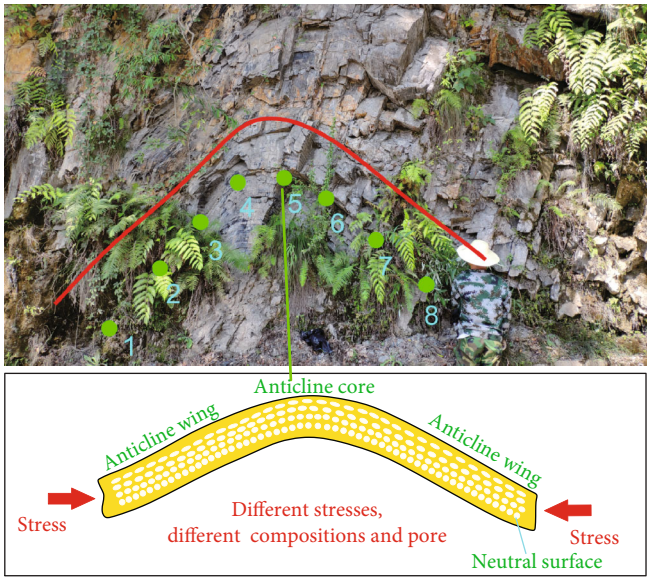

Figure 9: Stress distribution pattern of different structural parts of anticline. Modified from Ramsay and Huber [53].

are compact in the space around the brittle minerals and increase the heterogeneity of the shale. Due to the tectonism, the hydrothermal fluid is filled into the microfracture formed by the tectonic deformation, which also may cause the shale with strong deformation to have high quartz content [37].

4.2. Effect of Tectonism on Pore Characteristics. Tectonic stress may have destroyed the mesopores to macropores within the OM in the deformed area, while OM-hosted micropores are retained due to their greater mechanical resilience [33–35, 54]. And tectonism also can cause the shale to develop a "mylonite structure" in the cleavage domains, which has a pore system composed of nanoscale intergranular gap, lamella gap aggregate, and pore network, thus greatly increasing the specific surface area and adsorption capacity of the shale [32]. FE-SEM images show that strong deformed shale samples have more OM-hosted micropores (Figures 6(a)–6(d)). From the results of LPGA experiment, it can be found that strong deformed shale samples generally have a larger micropore specific surface area and a larger micropore volume (Figures 10(b) and 10(d)). Ju et al. also found that strong ductile deformation enables the pore size shift its distribution in shale, and a strong tectonic shear can improve the coal-bearing shale pore specific surface area [36]. These changes in pore characteristics are originated from the rheological behavior of the ductile minerals (clay minerals and OM). Tectonism can stretch the OM and fill the clay mineral layers to form more micropores (Figure 11, I). There is the presence of pressure shadows around the rigid grains (quartz, feldspar, dolomite, calcite, and pyrite) [33], which can resist the tectonic compression and also protect the surrounding OM pores (Figures 6(j) and 11, II).

During the compaction process, a large number of the interP pores and intraP pores can be destroyed; this is why

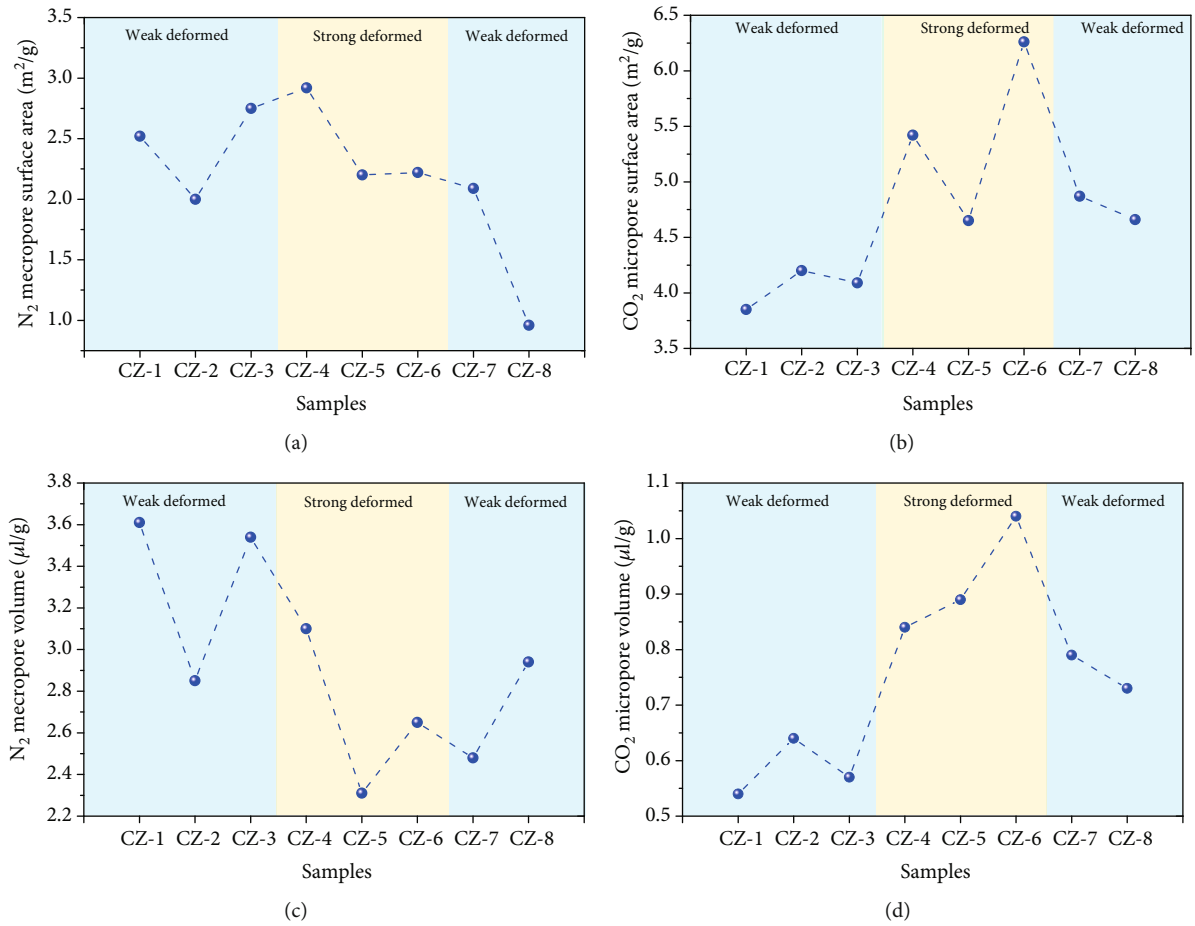

Figure 10: PV and SSA of the Lujiaping shale from the data of LPGA experiments.

the pore volume is reduced by up to 88% [49]. The late tectonic extrusion is essential to the interP pores and the intraP pores [23, 36, 37]. Although the intraP pores are relatively developed, considering the independent development and light connectivity of the intraP pores, they contribute less to the overall pore system [7, 13]. The most common interP pores are usually elongated strips along the edges of rigid grains (Figures 6(f) and 6(h)). Due to the dissolution, some small interP pores are formed at the edge of the rigid grains, ranging from a few tens to several hundreds of nanometers (Figure 6(e)–6(h)). The tectonism can cause the rigid grains to rotate and slide and further enlarge the dissolution pores at the rigid grains' edge (Figure 11, III). Tectonism can also cause some mesopores to become macropores; for example, tectonism can connect the interP pores at the rigid grains' edge to form microfractures (Figure 6(h)). Therefore, the sample with strong deformation has a larger mesopore specific surface area and a smaller mesopore volume (Figures 10(a) and 10(c)).

Shale deformation is classified in three main forms of brittle deformation, brittle-ductile deformation, and ductile deformation [36–40]. Whether it is brittle deformation or ductile deformation, as the deformation intensity increases, both microchannels and microfractures increase [37, 38, 40]. Compared with the development characteristics of microchannels and microfractures of shale samples with various deformation intensities, some points may be concluded that samples with strong deformation have more microchannels and microfractures (Figures 6(i)–6(l)). Through linking with microfractures, tectonism is able to form the microfracture system (Figure 11, IV). Although some microchannels and microfractures will close under tectonic stress, the principal stress of different directions in multiple phases will cause the microfractures to unfold again [23]. Most noteworthy is that these microfractures and microchannels also change the mechanical properties and migration capabilities of shale, which is more conducive to future development [51].

4.3. Effect of Tectonism on Pore Fractal. To characterize the complexity of the pore network in shale reservoirs, some researchers reach this goal in a way to calculate fractal dimensions [8, 11, 26, 45]. N_2 has different adsorption mechanisms under different pressure conditions, so the fractal dimension D_1 of the low pressure stage is usually used to indicate the surface roughness of the pore structure, while the fractal dimension D_2 of the high-pressure stage represents the irregularity of the pore structure [11, 47, 48]. The tectonism can change the relationship between the pores in the shale reservoir, making the pore system of the shale more complex [32, 36–40]. The samples with strong deformation generally have a relatively large D_1 and D_2 than samples with

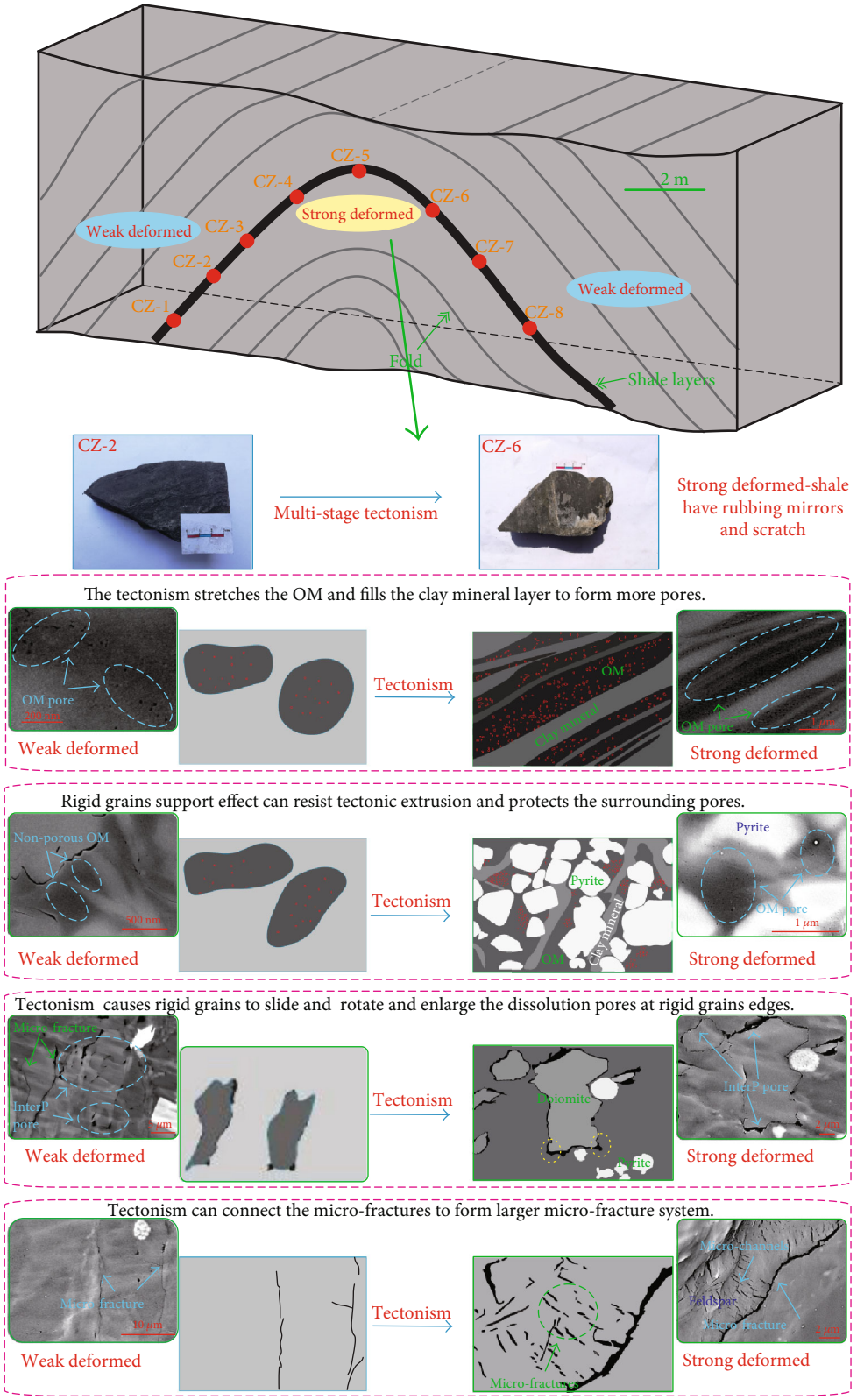

Figure 11: Evolution of pore structure in samples with different tectonic deformations.

weak deformation (Table 2 and Figure 12). The samples with strong deformation that always have a relatively large D_1 may be related to the mixing behavior of clay and OM. The OM-clay aggregate has many organic pores, and the organic pores have neither a smooth surface nor a regular shape, which also leads the shale with strong deformation having a large D_1.

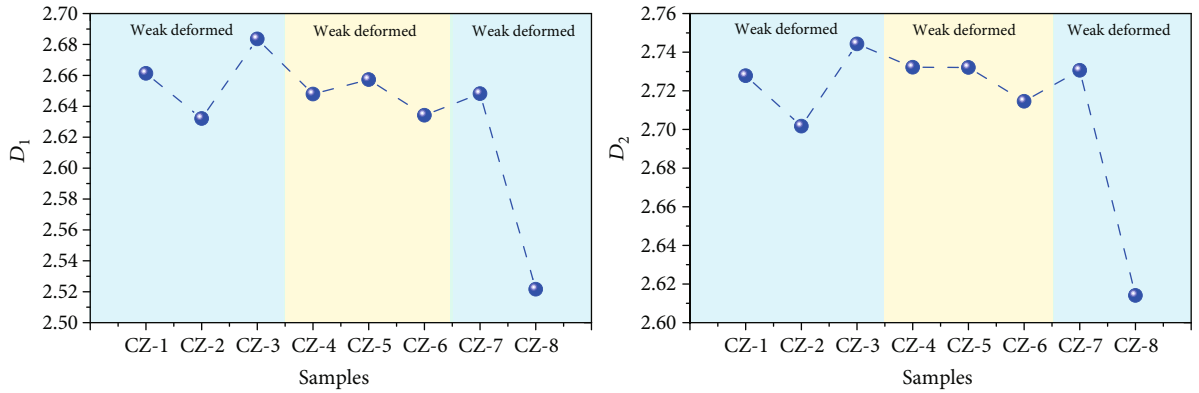

Figure 12: Fractal dimension of the Lujiaping shale from the data of LP-N_2-GA experiments.

The rough surface can also form some additional pores that increase the adsorption capacity of the shale. The irregularity of pore structure has an important influence on the spatial geometrical dimension, pore heterogeneity, and interconnectivity [11, 13, 49]. And multiple tectonism has an important influence on the pore network, which makes the nm-μm scale interP gap particularly developed [37, 40]. This also causes the shale with strong deformation to have a high D_2.

5. Conclusion

This paper mainly studies the effects of tectonics on the composition and pore characteristics of shale reservoirs. A series of experiments were carried out on 8 deformed shale samples from the Lujiaping Formation in the northeastern of Chongqing, including mineralogy, organic geochemistry, low-pressure N_2/CO_2 adsorption, and FE-SEM. The major conclusions of this paper are as follows:

(1) Tectonism has an important influence on the pores in the shale reservoir, especially OM pores, interP pores, microchannels, and microfractures. The strong deformed shale samples have more organic pores, larger interP pores, and more microfractures and microchannels

(2) The organic-clay aggregate produced by the tectonism provides more specific surface area and increases the adsorption capacity of the deformed shale. However, due to the tectonism, some micropores become macropores, which also leads the strong deformed shale to have a smaller mesopore volume

(3) Different structural parts have different stress environment, and different minerals have different mechanical properties, so different pore characteristics exist in different structural parts. Tectonism can cause the rheology of the clay mineral and OM around the rigid grains so that the rigid grains can protect the surrounding micropores. The tectonism can cause the rigid grains to slide and rotate and also enlarge the dissolution pores at the rigid grains' edge

(4) Tectonism makes the pore network in shale reservoirs more complex. The strong deformed samples generally have larger D_1 and D_2 than weak deformed samples. As the shale deformation intensity increases, the surface roughness and irregularity of the pore structure are enhanced

Data Availability

The original data used to support the findings of this study are available from the corresponding author (ymzhucumt@126.com) upon request.

Additional Points

Highlights. (1) The effects of tectonism on the composition of shale reservoirs are investigated to specify the mode of influence. (2) Analysis of the effect of tectonism on the composition is used for clarifying the influence of tectonism on the pore characteristics. (3) The tectonism will complicate the pore network in the shale reservoir as well as cast a crucial impact and have an important effect on the pore fractal dimension.

Conflicts of Interest

The authors declare that there are no conflicts of interest regarding the publication of this paper.

Acknowledgments

This research is sponsored by the National Natural Science Foundation of China (Project Nos. 41872132 and 41802183), National Science and Technology Major Project (Project No. 2017ZX05035004-002), and Scientific Research Foundation of Key Laboratory of Coalbed Methane Resources and Reservoir Formation Process Ministry of Education (China University of Mining and Technology) (No. 2019-008). We really appreciate the help from other experimenters in the Jiangsu Design Institute of Geology for Minerals Resources labs.

References

[1] J. B. Curtis, "Fractured shale-gas systems," *AAPG Bulletin*, vol. 86, no. 11, pp. 1921–1938, 2002.

[2] R. G. Loucks and S. C. Ruppel, "Mississippian Barnett Shale: lithofacies and depositional setting of a deep-water shale-gas succession in the Fort Worth Basin, Texas," *AAPG Bulletin*, vol. 91, no. 4, pp. 579–601, 2007.

[3] D. M. Jarvie, R. J. Hill, T. E. Ruble, and R. M. Pollastro, "Unconventional shale-gas systems: the Mississippian Barnett Shale of north-central Texas as one model for thermogenic shale-gas assessment," *AAPG Bulletin*, vol. 91, no. 4, pp. 475–499, 2007.

[4] F. Hao, H. Zou, and Y. Lu, "Mechanisms of shale gas storage: implications for shale gas exploration in China," *AAPG Bulletin*, vol. 97, no. 8, pp. 1325–1346, 2013.

[5] S. Chen, Y. Zhu, H. Wang, H. Liu, W. Wei, and J. Fang, "Shale gas reservoir characterisation: a typical case in the southern Sichuan Basin of China," *Energy*, vol. 36, no. 11, pp. 6609–6616, 2011.

[6] F. Yang, Z. Ning, and H. Liu, "Fractal characteristics of shales from a shale gas reservoir in the Sichuan Basin, China," *Fuel*, vol. 115, pp. 378–384, 2014.

[7] Y. Wang, Y. Zhu, S. Chen, and W. Li, "Characteristics of the nanoscale pore structure in northwestern Hunan shale gas reservoirs using field emission scanning electron microscopy, high-pressure mercury intrusion, and gas adsorption," *Energy & Fuels*, vol. 28, no. 2, pp. 945–955, 2014.

[8] H. Xu, W. Zhou, R. Zhang, S. Liu, and Q. Zhou, "Characterizations of pore, mineral and petrographic properties of marine shale using multiple techniques and their implications on gas storage capability for Sichuan Longmaxi gas shale field in China," *Fuel*, vol. 241, pp. 360–371, 2019.

[9] S. Chen, Y. Han, C. Fu, Zhang, Y. Zhu, and Z. Zuo, "Micro and nano-size pores of clay minerals in shale reservoirs: implication for the accumulation of shale gas," *Sedimentary Geology*, vol. 342, pp. 180–190, 2016.

[10] R. Yang, S. He, Q. Hu, M. Sun, D. Hu, and J. Yi, "Applying SANS technique to characterize nano-scale pore structure of Longmaxi shale, Sichuan Basin (China)," *Fuel*, vol. 197, pp. 91–99, 2017.

[11] Y. Wang, Y. Zhu, S. Liu, and R. Zhang, "Pore characterization and its impact on methane adsorption capacity for organic-rich marine shales," *Fuel*, vol. 181, pp. 227–237, 2016.

[12] Y. Wang, Y. Zhu, S. Liu, and R. Zhang, "Methane adsorption measurements and modeling for organic-rich marine shale samples," *Fuel*, vol. 172, article S001623611501340X, pp. 301–309, 2016.

[13] R. G. Loucks, R. M. Reed, S. C. Ruppel, and U. Hammes, "Spectrum of pore types and networks in mudrocks and a descriptive classification for matrix-related mudrock pores," *AAPG Bulletin*, vol. 96, no. 6, pp. 1071–1098, 2012.

[14] C. Zou, Y. Zhi, J. Dai et al., "The characteristics and significance of conventional and unconventional Sinian–Silurian gas systems in the Sichuan Basin, Central China," *Marine and Petroleum Geology*, vol. 64, article S0264817215000847, pp. 386–402, 2015.

[15] C. Zou, Y. Zhi, S. Pan et al., "Shale gas formation and occurrence in China: an overview of the current status and future potential," *Acta Geologica Sinica - English Edition*, vol. 90, no. 4, pp. 1249–1283, 2016.

[16] C. Zou, D. Dong, Y. Wang et al., "Shale gas in China: characteristics, challenges and prospects (I)," *Petroleum Exploration and Development*, vol. 42, no. 6, pp. 753–767, 2015.

[17] S. Chen, Y. Zhu, C. Si, H. Yufu, F. Changqing, and F. Junhua, "Hydrocarbon generation and shale gas accumulation in the Longmaxi Formation, Southern Sichuan Basin, China," *Marine and Petroleum Geology*, vol. 86, pp. 248–258, 2017.

[18] T. Guo, "Key geological issues and main controls on accumulation and enrichment of Chinese shale gas," *Petroleum Exploration and Development*, vol. 43, no. 3, pp. 349–359, 2016.

[19] T. Guo and H. Zhang, "Formation and enrichment mode of Jiaoshiba shale gas field, Sichuan basin," *Petroleum Exploration and Development*, vol. 41, no. 1, pp. 31–40, 2014.

[20] X. Wei, Y. Li, Z. Wei, R. Liu, G. Yu, and Q. Wang, "Effects of preservation conditions on enrichment and high yield of shale gas in Sichuan Basin and its periphery," *Petroleum Geology & Experiment*, vol. 39, no. 2, pp. 147–153, 2017.

[21] J. Tang, Y. Li, K. Wang, and Q. Zeyu, "Comprehensive evaluation of effective preservation zone of Longmaxi Formation shale gas in the Southeast Sichuan Basin," *Natural Gas Industry*, vol. 35, no. 5, pp. 15–23, 2015.

[22] T. Zhang, H. Yin, D. Gu et al., "Structural deformation characteristics and shale gas preservation of lower Yangtze region," *Journal of China Coal Society*, vol. 38, no. 5, pp. 883–889, 2013.

[23] H. Li, *Effect of Tectonic Compression on the Characteristics of Pore Structure and Gas Storage of Shale*, Guangzhou Institute of Geochemistry, Chinese Academy of Sciences, Guangzhou, 2017.

[24] N. Peng, S. He, F. Hao et al., "The pore structure and difference between Wufeng and Longmaxi Shales in Pengshui Area, Southeastern Sichuan," *Earth Science*, vol. 42, no. 7, pp. 1134–1146, 2017.

[25] B. Zan, S. Liu, Z. Bai, B. Ran, Y. Ye, and J. Qiu, "Pore characteristics of shale gas reservoir of Longmaxi Formation in Weiyuan Area, southwest of Sichuan Basin," *Geological Science and Technology Information*, vol. 2, pp. 65–74, 2017.

[26] Y. Peng and Y. Zhu, "Effect of extrusion stress on porosity of Longmaxi Formation shale in East Sichuan and South Chongqing," *Special Oil & Gas Reservoirs*, vol. 23, no. 2, pp. 132–135, 2016.

[27] X. Xie, F. Hao, Y. Lu et al., "Differential enrichment mechanism and key technology of shale gas in complex areas of South China," *Earth Science*, vol. 42, no. 7, pp. 1045–1056, 2017.

[28] J. Sun and B. Luo, "Differential enrichment mechanism and key technology of shale gas in complex areas of South China," *Oil and Gas Geology*, vol. 37, no. 6, pp. 809–818, 2016.

[29] T. Borjigin, S. Baojian, Y. Lingjie et al., "Mechanisms of shale gas generation and accumulation in the Ordovician Wufeng-Longmaxi Formation, Sichuan Basin, SW China," *Petroleum Exploration and Development*, vol. 44, no. 1, pp. 69–78, 2017.

[30] X. Liu, D. Song, X. He, Z. Wang, M. Zeng, and K. Deng, "Nanopore structure of deep-burial coals explored by AFM," *Fuel*, vol. 246, pp. 9–17, 2019.

[31] Y. Wang, C. Li, J. Hao, and R. Q. Zhou, "X-ray microtomography for investigation of meso-structural changes and crack evolution in Longmaxi formation shale during compressive deformation," *Journal of Petroleum Science and Engineering*, vol. 164, pp. 278–288, 2018.

[32] Y. Ma, N. Zhong, D. Li, Z. Pan, L. Cheng, and K. Liu, "Organic matter/clay mineral intergranular pores in the Lower Cambrian Lujiaping shale in the north-eastern part of the upper

Yangtze area, China: a possible microscopic mechanism for gas preservation," *International Journal of Coal Geology*, vol. 137, article S0166516214002262, pp. 38–54, 2015.

[33] J. Schieber, "Common themes in the formation and preservation of intrinsic porosity in shales and mudstones - illustrated with examples across the Phanerozoic," in *SPE Unconventional Gas Conference*, Pittsburgh, PA, USA, 2010.

[34] A. Deirieh, I. Y. Chang, B. Casey, D. Joester, and J. T. Germaine, "Impact of drying and effective stresses on the pore space and microstructure of Mudrocks," *Journal of Geophysical Research: Solid Earth*, vol. 124, no. 5, pp. 4290–4304, 2019.

[35] R. M. Bustin, A. M. M. Bustin, A. Cui, D. Ross, and V. M. Pathi, "Impact of shale properties on pore structure and storage characteristics," in *SPE Shale Gas Production Conference*, Fort Worth, TX, USA, 2008.

[36] Y. Ju, Y. Sun, J. Tan et al., "The composition, pore structure characterization and deformation mechanism of coal-bearing shales from tectonically altered coalfields in eastern China," *Fuel*, vol. 234, pp. 626–642, 2018.

[37] H. Zhu, Y. Ju, Q. Yu, C. Huang, and L. Zhang, "Impact of tectonism on pore type and pore structure evolution in organic-rich shale: implications for gas storage and migration pathways in naturally deformed rocks," *Fuel*, vol. 228, pp. 272–289, 2018.

[38] M. Liang, Z. Wang, L. Gao, C. Li, and H. Li, "Evolution of pore structure in gas shale related to structural deformation," *Fuel*, vol. 197, pp. 310–319, 2017.

[39] H. Zhu, Y. Ju, C. Huang et al., "Pore structure variations across structural deformation of Silurian Longmaxi shale: an example from the Chuandong Thrust-Fold Belt," *Fuel*, vol. 241, pp. 914–932, 2019.

[40] Z. Li, Z. Jiang, Z. Liang, H. Yu, and Y. Yang, "Pore-structure characterisation of tectonically deformed shales: a case study of Wufeng-Longmaxi Formation in western Hunan Province, southern China," *Australian Journal of Earth Sciences*, vol. 66, no. 7, pp. 1075–1084, 2019.

[41] J. Hu, H. Chen, H. Qu, G. Wu, J. Yang, and Z. Zhang, "Mesozoic deformations of the Dabashan in the southern Qinling orogen, central China," *Journal of Asia Earth Sciences*, vol. 47, pp. 171–184, 2012.

[42] W. Shi, Y. Zhang, S. Dong et al., "Intra-continental Dabashan orocline, southwestern Qinling, central China," *Journal of Asia Earth Sciences*, vol. 46, pp. 20–38, 2012.

[43] N. Zhong and Y. Qin, *Organic Petrology of Carbonate Rocks: Characteristics, Origin and Evolution of Macerals with Respects to Hydrocarbon Generation*, Science Press, Bingjing, 1995.

[44] N. Peng, S. He, Q. Hu et al., "Organic nanopore structure and fractal characteristics of Wufeng and lower member of Longmaxi shales in southeastern Sichuan, China," *Marine and Petroleum Geology*, vol. 103, pp. 456–472, 2019.

[45] X. Li, S. Chen, X. Wang, Y. Zhu, M. Chang, and C. Uwamahoro, "Pore structure heterogeneity of the Xiamaling formation shale gas reservoir in the Yanshan area of China: evaluation of geological controlling factors," *Acta Geologica Sinica - English Edition*, vol. 93, no. 3, pp. 588–603, 2019.

[46] Y. Cai, D. Liu, Z. Pan, Y. Yao, J. Li, and Y. Qiu, "Pore structure and its impact on CH_4 adsorption capacity and flow capability of bituminous and subbituminous coals from Northeast China," *Fuel*, vol. 103, pp. 258–268, 2013.

[47] D. Avnir and M. Jaroniec, "An isotherm equation for adsorption on fractal surfaces of heterogeneous porous materials," *Langmuir*, vol. 5, no. 6, pp. 1431–1433, 1989.

[48] T. Vaimakis, C. Skordilis, and P. Pomonis, "Alternation of geometrical and fractal dimensions of phosphate ore particles during grinding," *Journal of Colloid and Interface Science*, vol. 172, no. 2, pp. 311–316, 1995.

[49] C. R. Clarkson, N. Solano, R. M. Bustin et al., "Pore structure characterization of North American shale gas reservoirs using USANS/SANS, gas adsorption, and mercury intrusion," *Fuel*, vol. 103, pp. 606–616, 2013.

[50] H. Han, N. Zhong, Y. Ma et al., "Gas storage and controlling factors in an over-mature marine shale: A case study of the Lower Cambrian Lujiaping shale in the Dabashan arc-like thrust- fold belt, southwestern China," *Journal of Natural Gas Science and Engineering*, vol. 33, pp. 839–853, 2016.

[51] A. Ougier-Simonin, F. Renard, C. Boehm, and S. Vidal-Gilbert, "Microfracturing and microporosity in shales," *Earth Science Reviews*, vol. 162, pp. 198–226, 2016.

[52] S. Zhou and Z. Lu, "A study of the secondary pore space in the Cretaceous reservoir in the west slope in Songliao Basin," *Petroleum Expoloration and Development*, vol. 5, p. 2, 1989.

[53] J. G. Ramsay and M. I. Huber, *The techniques of modern structural geology: folds and fractures*, Academic Press, 1987.

[54] Y. Ma, O. H. Ardakani, N. Zhong et al., "Possible pore structure deformation effects on the shale gas enrichment: an example from the Lower Cambrian shales of the Eastern Upper Yangtze Platform, South China," *International Journal of Coal Geology*, vol. 217, article 103349, 2020.